NACA TN No. 1624

8117

NATIONAL ADVISORY COMMITTEE FOR AERONAUTICS

TECHNICAL NOTE

No. 1624

TWO-DIMENSIONAL WIND-TUNNEL INVESTIGATION OF AN NACA 64-009 AIRFOIL EQUIPPED WITH TWO TYPES OF LEADING-EDGE FLAP

By Felicien F. Fullmer, Jr.

Langley Memorial Aeronautical Laboratory
Langley Field, Va.

Washington
June 1948

NATIONAL ADVISORY COMMITTEE FOR AERONAUTICS

TECHNICAL NOTE NO. 1624

TWO-DIMENSIONAL WIND-TUNNEL INVESTIGATION OF AN NACA 64-009 AIRFOIL EQUIPPED WITH TWO TYPES OF LEADING-EDGE FLAP

By Felicien F. Fullmer, Jr.

SUMMARY

An investigation was made to determine the effect of leading-edge flaps on the maximum lift coefficient of an NACA 64-009 airfoil and to compare the results with data obtained from previous tests of similarly shaped flaps on an NACA 64_1-012 airfoil (NACA TN No. 1277). The investigation included tests of two 10-percent-chord leading-edge flaps, one intended to slide forward along the upper surface and the other hinged at the center of the airfoil leading-edge radius and deflecting from the lower surface. The flaps were tested on the plain airfoil and on the airfoil with a trailing-edge split flap deflected 60°. Data are given to show the section lift characteristics for a range of flap deflection and the section pitching-moment and lift characteristics with leading-edge roughness for the optimum flap arrangements.

The results indicate that the upper-surface leading-edge flap was, in general, a more effective high-lift device than the lower-surface leading-edge flap, especially when used alone on the plain airfoil. A leading-edge flap of a given size and shape was found to be capable, in general, of producing (for approx. equal amounts of effective camber) the same or slightly greater increments in the maximum lift coefficient when attached to the 9-percent-thick airfoil rather than to the 12-percent-thick airfoil.

In addition, it was found that deflecting either type of leading-edge flap resulted in a forward movement of the aerodynamic center at high angles of attack. With regard to the effects of surface roughness, the upper-surface leading-edge flap was equally as good as the lower-surface leading-edge flap even though the decrement in maximum section lift coefficient due to roughness was larger for the upper-surface leading-edge-flap arrangement.

INTRODUCTION

The problem of obtaining adequate maximum lift coefficients on highly swept wings has shown the need for a more thorough investigation of all types of leading-edge auxiliary high-lift devices. Considerable interest has recently developed in one of these devices, the leading-edge flap, because it has possibilities as a high-lift device for use on highly swept wings, for any wing on which the normal trailing-edge high-lift devices are ineffective, or for thin wings on which the proven types of high-lift devices cannot be installed because of limited thickness near the trailing edge.

The leading-edge-flap investigation conducted by the National Advisory Committee for Aeronautics and reported in reference 1 was undertaken primarily to verify results obtained at the Deutsche Versuchsanstalt für Luftfahrt and reported by Köster and Krüger in references 2 and 3, respectively. The initial investigation, therefore, was limited to tests on one airfoil similar in thickness and thickness distribution to that used in the investigations of references 1 and 2. The results (reference 1), in general, verified those obtained by Köster and Krüger and showed that substantial increases in the maximum lift coefficient accompanied by increases in the angle of attack for maximum lift could be obtained by the use of leading-edge flaps on the NACA 64_1-012 airfoil section.

The present investigation was made in order to determine the effect of leading-edge flaps on the maximum lift coefficients of a thinner airfoil. In order to correlate changes in flap effectiveness with changes in airfoil thickness, the leading-edge flaps used for the present tests were similar in size and shape to those previously tested (reference 1) and were fitted to the airfoil in such a manner as to obtain as closely as possible the camber of the best configuration previously tested in reference 1.

The investigation, conducted in the Langley two-dimensional low-turbulence pressure tunnel, included tests of an NACA 64-009 airfoil equipped with a lower-surface flap hinged at the airfoil leading edge and an extensible type of upper-surface leading-edge flap. Both types of flap were tested individually and in combination with a trailing-edge split flap.

SYMBOLS

α_o airfoil section angle of attack

c_l airfoil section lift coefficient (l/qc)

$c_{l_{max}}$ maximum section lift coefficient

$c_{m_{c/4}}$ airfoil section pitching-moment coefficient about quarter-chord point of plain airfoil $\left(\frac{m_{c/4}}{qc^2}\right)$

$\Delta\alpha_o$ increment of section angle of attack for maximum section lift coefficient due to leading-edge-flap deflection

$\Delta c_{l_{max}}$ increment of maximum section lift coefficient due to leading-edge-flap deflection

$\delta_{f_{L.E.}}$ deflection of leading-edge flap, measured in clockwise direction from the airfoil chord (zero when flap lies along surface), degrees

$\delta_{f_{T.E.}}$ deflection of trailing-edge flap, positive when flap trailing edge moves downward, degrees

c chord of plain airfoil

R Reynolds number

l lift per unit span

$m_{c/4}$ moment per unit span about quarter-chord point of plain airfoil

q dynamic pressure

MODEL

The model, which was constructed of steel, had a chord of 24 inches, a span of 35.5 inches, and was built to the contour of the NACA 64-009 airfoil. (See table I.) The 20-percent-chord trailing-edge split flap, set at a deflection of 60° and used for some of these tests, was simulated by a prismatic block of laminated mahogany attached to the lower surface of the model as shown in figure 1(a).

The 10-percent-chord upper-surface flap used for these tests simulated an extensible type of flap which, when retracted, was intended to form an integral part of the airfoil leading edge and upper surface. The profile of the first 45 percent of the flap was identical in contour to that of the plain airfoil from the leading edge to the 4.5-percent-wing-chord station, and the remaining 55 percent of the flap was of true circular-arc contour. The flap could thus be extended by sliding it along a circular-arc track. The radius used to describe this circular arc and the location of the center of curvature were chosen so that the arc conformed to the contour of the airfoil upper surface between the 1.25-percent-chord and 4.5-percent-chord stations of the airfoil. Because the arc described by this radius formed a part of the original airfoil surface, the flap, when extended, faired smoothly into the airfoil upper surface to produce a highly cambered airfoil as shown in figure 1. The sketches (fig. 2) show the ordinates, the relation of the flap to the model, and the method of measuring the effective 10-percent chord of the flap.

The lower-surface leading-edge flap was designed to rotate about a single fixed pivot which was coincident with the location of the center of the airfoil leading-edge radius. The flap had a chord equal to 10 percent of the airfoil chord, a shape which conformed to the contour of the airfoil from the 0-percent-chord to the 9.4-percent-chord airfoil stations, and a leading-edge radius equal to 0.6 percent of the airfoil chord. Photographs of this flap attached to the airfoil with and without the trailing-edge split flap are presented in figure 3. A sketch showing the flap shape and the location of the flap relative to the airfoil is shown in figure 4.

Both leading-edge flaps were constructed of $\frac{1}{16}$-inch sheet iron and were attached to the model by six brackets equally spaced across the 35.5-inch span of the model. The deflection of each leading-edge flap was measured in a clockwise direction (figs. 2 and 4) from the airfoil chord.

Leading-edge roughness used for the tests of the plain airfoil and the airfoil trailing-edge-flap configuration consisted of 0.01-inch carborundum grains shellacked to the airfoil upper and lower surfaces for a distance equal to 8 percent of the chord measured along the surfaces from the airfoil leading edge. The roughness used for the tests of the leading-edge-flap configurations consisted of similar size carborundum grains shellacked to the flap leading edge and to the forward 80 percent of the flap upper surface. (See fig. 3(a).)

METHODS AND TESTS

The tests were made in the Langley two-dimensional low-turbulence pressure tunnel. The methods used to obtain and to correct the data for wind-tunnel-wall constriction and for the additional blocking effect of the model at high angles of attack are fully explained in reference 4.

The lift characteristics were obtained for the model with each of the leading-edge flaps alone and in combination with the trailing-edge split flap deflected 60°. The pitching-moment characteristics for the model in a smooth condition and the lift characteristics for the model in a rough condition are presented only for the most favorable flap settings of the various airfoil flap configurations. All tests were made at a density of 0.0096 slug per cubic foot and at a dynamic pressure of approximately 70 pounds per square foot. These values correspond to a Reynolds number of 6.0×10^6 and a Mach number of 0.12.

ACCURACY OF DATA

The probable error in individual test points as determined from check tests, consideration of the sensitivity of the measuring instruments, and the departure of points from the faired curves is estimated to be within the following limits:

Over the linear portion of the lift curve:

c_l	±0.005
$c_{m_{c/4}}$	±0.002
α_o, degree	±0.1

Near maximum lift coefficient:

c_l	±0.020
$c_{m_{c/4}}$	±0.010
α_o, degree	±0.10

RESULTS AND DISCUSSION

The section lift characteristics obtained from tests of the various airfoil flap configurations are presented in figures 5 to 7. The variation of the increment of maximum section lift coefficient $\Delta c_{l_{max}}$ and of the increment of section angle of attack for maximum section lift coefficient $\Delta\alpha_o$ with leading-edge-flap deflection is presented in figure 8. The section pitching-moment characteristics of the plain airfoil, of the airfoil trailing-edge-flap arrangement, and of the optimum airfoil leading-edge-flap arrangements tested are presented in figure 9. The effect of leading-edge roughness on the section lift characteristics of the airfoil with various arrangements of leading-edge and trailing-edge flaps is shown in figure 10.

Lift Characteristics

The data presented in figures 5 to 7 show that leading-edge flaps of the type tested increased the maximum section lift coefficient and also the section angle of attack at which the maximum lift coefficient occurs. The maximum section lift coefficients, the angles of attack at which the maximum section lift coefficients occurred, and the increments that were obtained for the various optimum configurations are summarized in table II. For purposes of comparison, the results obtained from tests of an NACA 64_1-012 airfoil equipped with similar flap arrangements (reference 1) are also presented in table II.

The leading-edge flap produces the greater part of these increases in $c_{l_{max}}$ and in the angle of attack for $c_{l_{max}}$ by reducing the magnitude of the pressure peaks and the magnitude of the adverse pressure gradient usually associated with the flow conditions near maximum lift of the airfoil. Some of the increase in lift is, of course, also associated with the effective increase in area caused by the flap deflection. A more complete discussion of the manner in which the leading-edge-flap installation produces these changes in the airfoil flap aerodynamic characteristics is given in reference 1.

Upper-surface flap.- The section lift characteristics are presented in figure 5. The maximum lift coefficient, the angle of attack for $c_{l_{max}}$, and the increments $\Delta c_{l_{max}}$ and $\Delta \alpha_0$ are summarized in table II. A comparison of these results with those of reference 1 (also given in table II) shows that the maximum lift coefficients of the 9-percent-thick and 12-percent-thick airfoil sections with the trailing-edge flap off were essentially the same for approximately equal deflections of the leading-edge flap. The increment of maximum section lift coefficient $\Delta c_{l_{max}}$ for the 9-percent-thick airfoil, however, was nearly twice as great as that obtained for the 12-percent-thick airfoil. This variation in $\Delta c_{l_{max}}$ results from the differences in the maximum lift coefficients of the two airfoils with flaps neutral. The flaps were similar in size and shape and the effective camber of both airfoils with flaps deflected was approximately the same; however, the upper-surface leading-edge flap was more effective as a high-lift device on the 9-percent-thick airfoil than on the 12-percent-thick airfoil.

An examination of the results (table II) obtained from the leading-edge flaps when tested in conjunction with the trailing-edge split flaps shows that the difference (0.34) in $c_{l_{max}}$ of the 9-percent-thick and 12-percent-thick airfoils was approximately the same as the difference (0.37) in $c_{l_{max}}$ of the airfoils with the trailing-edge split flaps alone. Since the corresponding increments in $c_{l_{max}}$ resulting from the installation of the leading-edge flap on either the 9-percent-thick airfoil or the 12-percent-thick airfoil were about the same (0.84 and 0.81, respectively), it can be concluded that this leading-edge flap was equally effective on both airfoils. However, when the trailing-edge flap was deflected on the NACA 64-009 airfoil, the effectiveness of the leading-edge flap did not increase so much as it did in the tests of the NACA 64_1-012 airfoil section.

Lower-surface flap.- The section lift characteristics are presented in figures 6 and 7. The maximum lift coefficient, the angle of attack for $c_{l_{max}}$, and the increments $\Delta c_{l_{max}}$ and $\Delta \alpha_0$ are summarized in table II.

Because the lower-surface leading-edge flap was located at a more favorable position on the 9-percent-thick airfoil than the similar flap used on the 12-percent-thick airfoil of reference 1, no direct comparisons can be made between the two airfoil leading-edge-flap configurations. However, inasmuch as this lower-surface leading-edge-flap installation is similar to the upper-surface leading-edge-flap installation used on both the 9-percent-thick and 12-percent-thick airfoils, all comparisons will be made with respect to these upper-surface leading-edge flaps.

A comparison of the results obtained from tests of the lower-surface leading-edge flap on the NACA 64-009 airfoil with those obtained from tests of the upper-surface leading-edge flap on the NACA 64_1-012 airfoil (table II) shows that the lower-surface leading-edge flap on the 9-percent-thick airfoil, when used alone or in combination with the trailing-edge split flap, was capable of producing increments in $c_{l_{max}}$ and α_0 which were slightly higher than those which could be obtained with the upper-surface leading-edge flap used on the 12-percent-thick airfoil. As a high lift device, therefore, either the upper-surface or lower-surface leading-edge flap was more effective on the thinner airfoil.

The data presented in figure 8, for the NACA 64-009 airfoil, show that the increments in $c_{l_{max}}$ and α_0 due to deflection of the lower-surface leading-edge flap on the plain airfoil were not so large as those obtained with the upper-surface leading-edge flap, even though the effective camber of the airfoil with the flaps deflected was somewhat greater for the lower-surface leading-edge-flap configuration. This smaller increment in $c_{l_{max}}$ is thought to be attributable to the discontinuity in general contour of the upper surface at the point of intersection of the flap and the airfoil (fig. 4) and to the smaller curvature of this lower-surface type of flap, especially near the flap leading edge. An examination of the data obtained when the lower-surface leading-edge flap was used in conjunction with the split trailing-edge flap shows that the increments in $c_{l_{max}}$ and α_0 were about the same as those obtained from similar tests of the upper-surface leading-edge flap. Thus, the upper-surface leading-edge flap, when used on the plain NACA 64-009 airfoil, was more effective than the lower-surface leading-edge flap; either flap, however, was equally effective as a lift augmenter when used on the airfoil with the trailing-edge flap deflected 60°.

Pitching-Moment Characteristics

A comparison of the section pitching-moment data obtained for the NACA 64-009 airfoil with various arrangements of the leading-edge and trailing-edge flaps (fig. 9) shows that the addition of either leading-edge flap caused the pitching-moment coefficients to increase negatively with increasing lift coefficient until the angle of attack was approximately high enough for the flap to become effective. As the lift coefficient is increased beyond this point, the pitching-moment coefficients increase positively in a manner corresponding to a forward position of the aerodynamic center with respect to the quarter-chord point of the plain airfoil. Such a forward position of the aerodynamic center is consistent with the fact that area has been added ahead of the leading edge of the plain airfoil. The forward shift in the aerodynamic center was slightly larger for the upper-surface-flap installation than for the lower-surface-flap installation. The results show that the increments in pitching-moment coefficients which were obtained from the addition of either of the leading-edge flaps are relatively small in comparison with the increments resulting from deflection of the conventional split trailing-edge flap.

A comparison of the present results with those of reference 1 shows, in general, that the character of the pitching-moment curves with leading-edge flaps deflected was about the same for both airfoils. The magnitude of the coefficients and the slopes of the curves for the upper-surface leading-edge flap on the 12-percent-thick airfoil were slightly greater than those obtained for either the upper-surface or lower-surface leading-edge flaps on the 9-percent-thick airfoil.

Effects of Leading-Edge Roughness

The effect of roughness on the lift characteristics of the NACA 64-009 airfoil with various arrangements of leading-edge and trailing-edge flaps is presented in figure 10. The decrements in $c_{l_{max}}$ caused by the addition of roughness to the leading-edge flap were approximately 0.4 when the upper-surface leading-edge flap was used alone and approximately 0.2 when it was used in combination with the trailing-edge split flap. (See fig. 10(a).) The corresponding decrements in the maximum lift coefficient for the lower-surface leading-edge flap in the rough condition (fig. 10(b)) were about 0.2 when the leading-edge flap was used either alone or in conjunction with the trailing-edge split flap.

Although the decrements in maximum section lift coefficient caused by leading-edge roughness varied with the type of flap, the actual value (rough condition) of the maximum section lift coefficient was approximately the same for both leading-edge-flap installations. This condition existed whether the leading-edge flaps were tested on the plain airfoil or on the airfoil equipped with the trailing-edge split flap. From these results and the fact that the highest maximum lift coefficients (smooth condition) were obtained with the upper-surface leading-edge flap, it can be concluded that the upper-surface leading-edge-flap installation was equally as good, with regard to the effects of surface roughness, as the lower-surface leading-edge-flap installation even though the decrement in $c_{l_{max}}$ due to flap leading-edge roughness was larger for the upper-surface-flap arrangement.

A comparison of these results with those obtained for the upper-surface leading-edge-flap configurations on the NACA 64_1-012 airfoil (reference 1) shows that the decrement in maximum lift for the upper-surface leading-edge flap when used alone was the same for both airfoils. When the upper-surface or lower-surface leading-edge flap was used in combination with the trailing-edge flap, however, or when the lower-surface leading-edge flap was used alone on the NACA 64-009 airfoil, the decrement in $c_{l_{max}}$ was only one-half as large when the flaps were installed on the 9-percent-thick airfoil rather than on the 12-percent-thick airfoil. This result indicates, in general, that either type of leading-edge flap was less sensitive to roughness when it was installed on the 9-percent-thick airfoil.

CONCLUSIONS

An investigation, conducted at a Reynolds number of 6.0×10^6, was made to determine the effect of leading-edge flaps on the maximum lift coefficient of an NACA 64-009 airfoil and to compare the results with data obtained from previous tests of similarly shaped flaps on an NACA 64_1-012 airfoil. The results of these tests show that:

1. The upper-surface leading-edge flap was, in general, a more effective high-lift device than the lower-surface leading-edge flap, especially when used alone on the plain airfoil.

2. A leading-edge flap of a given size and shape was capable, in general, of producing (for approx. equal amounts of effective camber) the same or slightly larger increments in the maximum lift coefficient when attached to the 9-percent-thick airfoil rather than to the 12-percent-thick airfoil.

3. The deflection of either type of leading-edge flap resulted in a forward movement of the aerodynamic center at high angles of attack.

4. The upper-surface leading-edge flap was equally as good, with regard to the effects of surface roughness, as the lower-surface leading-edge flap even though the decrement in maximum section lift coefficient due to roughness was larger for the upper-surface leading-edge-flap arrangement.

Langley Memorial Aeronautical Laboratory
National Advisory Committee for Aeronautics
Langley Field, Va., February 19, 1948

REFERENCES

1. Fullmer, Felicien F., Jr.: Two-Dimensional Wind-Tunnel Investigation of the NACA 64_1-012 Airfoil Equipped with Two Types of Leading-Edge Flap. NACA TN No. 1277, 1947.

2. Köster, H.: Messungen am Profil $NACA_E$ 0 00 12 – 0,55 45 mit Spreiz- und Nasenspreizklappe. UM Nr. 1317, Deutsche Luftfahrtforschung (Berlin-Aldershof), 1944.

3. Krüger, W.: Systematische Windkanalmessungen an einem Laminarflügel mit Nasenklappe. Forschungsbericht Nr. 1948, Deutsche Luftfahrtforschung (Gottingen), 1944.

4. von Doenhoff, Albert E., and Abbott, Frank T., Jr.: The Langley Two-Dimensional Low-Turbulence Pressure Tunnel. NACA TN No. 1283, 1947.

TABLE I

ORDINATES FOR NACA 64-009 AIRFOIL

[Stations and ordinates given in percent of airfoil chord]

Upper surface		Lower surface	
Station	Ordinate	Station	Ordinate
0	0	0	0
.5	.739	.5	-.739
.75	.892	.75	-.892
1.25	1.128	1.25	-1.128
2.5	1.533	2.5	-1.533
4.5	2.009	4.5	-2.009
5.0	2.109	5.0	-2.109
7.5	2.543	7.5	-2.543
10.0	2.898	10.0	-2.898
15.0	3.455	15.0	-3.455
20.0	3.868	20.0	-3.868
25.0	4.170	25.0	-4.170
30.0	4.373	30.0	-4.373
35.0	4.479	35.0	-4.479
40.0	4.490	40.0	-4.490
45.0	4.364	45.0	-4.364
50.0	4.136	50.0	-4.136
55.0	3.826	55.0	-3.826
60.0	3.452	60.0	-3.452
65.0	3.026	65.0	-3.026
70.0	2.561	70.0	-2.561
75.0	2.069	75.0	-2.069
80.0	1.564	80.0	-1.564
85.0	1.069	85.0	-1.069
90.0	.611	90.0	-.611
95.0	.227	95.0	-.227
100	0	100	0
L. E. radius: 0.579			

NACA

TABLE II

SUMMARY OF RESULTS OBTAINED FROM TESTS OF THE NACA 64–009

AND THE NACA 64_1–012 AIRFOILS EQUIPPED WITH

TWO TYPES OF LEADING-EDGE FLAP

Model configuration	$c_{l_{max}}$	α_o (deg)	$\Delta c_{l_{max}}$	$\Delta\alpha_o$ (deg)	$\delta_{f_{L.E.}}$ (deg)	$\delta_{f_{T.E.}}$ (deg)
NACA 64–009 airfoil						
Airfoil alone	1.09	10.6	------	-----	------	------
Airfoil and lower-surface leading-edge flap	1.66	16.2	0.57	5.6	120	------
Airfoil and upper-surface leading-edge flap	1.82	17.8	.73	7.2	151.5	------
Airfoil and trailing-edge flap alone	1.80	5.5	------	-----	------	60
Airfoil trailing-edge flap and lower-surface leading-edge flap	2.61	14.2	.81	8.7	120	60
Airfoil trailing-edge flap and upper-surface leading-edge flap	2.64	14.2	.84	8.7	151.5	60
NACA 64_1–012 airfoil[a]						
Airfoil alone	1.42	14.3	------	-----	------	------
Airfoil and lower-surface leading-edge flap	1.54	15.7	0.12	1.4	120	------
Airfoil and upper-surface leading-edge flap	1.85	18.3	.43	4.0	153	------
Airfoil and trailing-edge flap alone	2.17	9.3	------	-----	------	60
Airfoil trailing-edge flap and lower-surface leading leading-edge flap	2.60	13.2	.43	3.9	112	60
Airfoil trailing-edge flap and upper-surface leading-edge flap	2.98	16.2	.81	6.9	153	60

[a]Data obtained from table in text of reference 1.

NACA

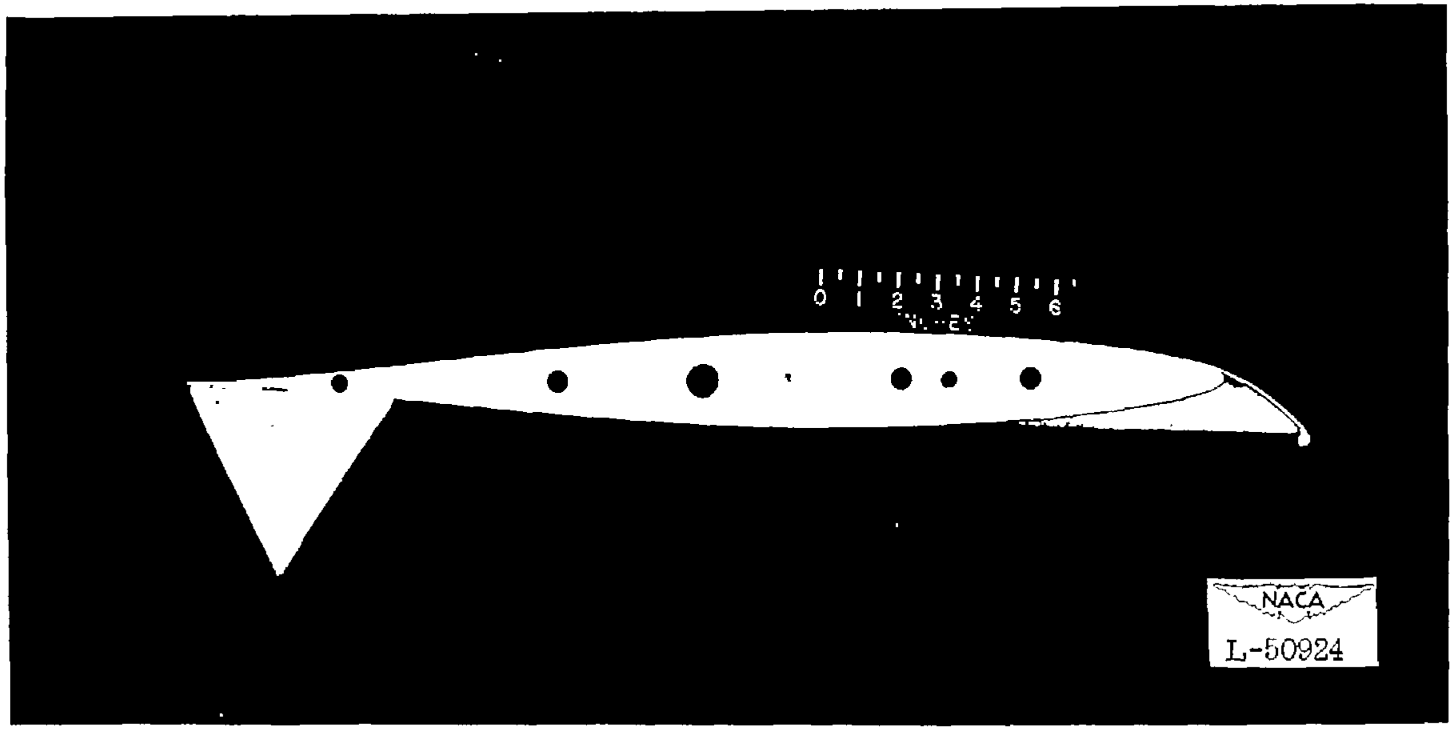

(a) Side view of the model showing installation of upper-surface leading-edge flap and lower-surface trailing-edge flap.

Figure 1.- Photographs of the NACA 64-009 airfoil section with the 0.10c upper-surface leading-edge flap alone and in combination with the 0.20c trailing-edge split flap.

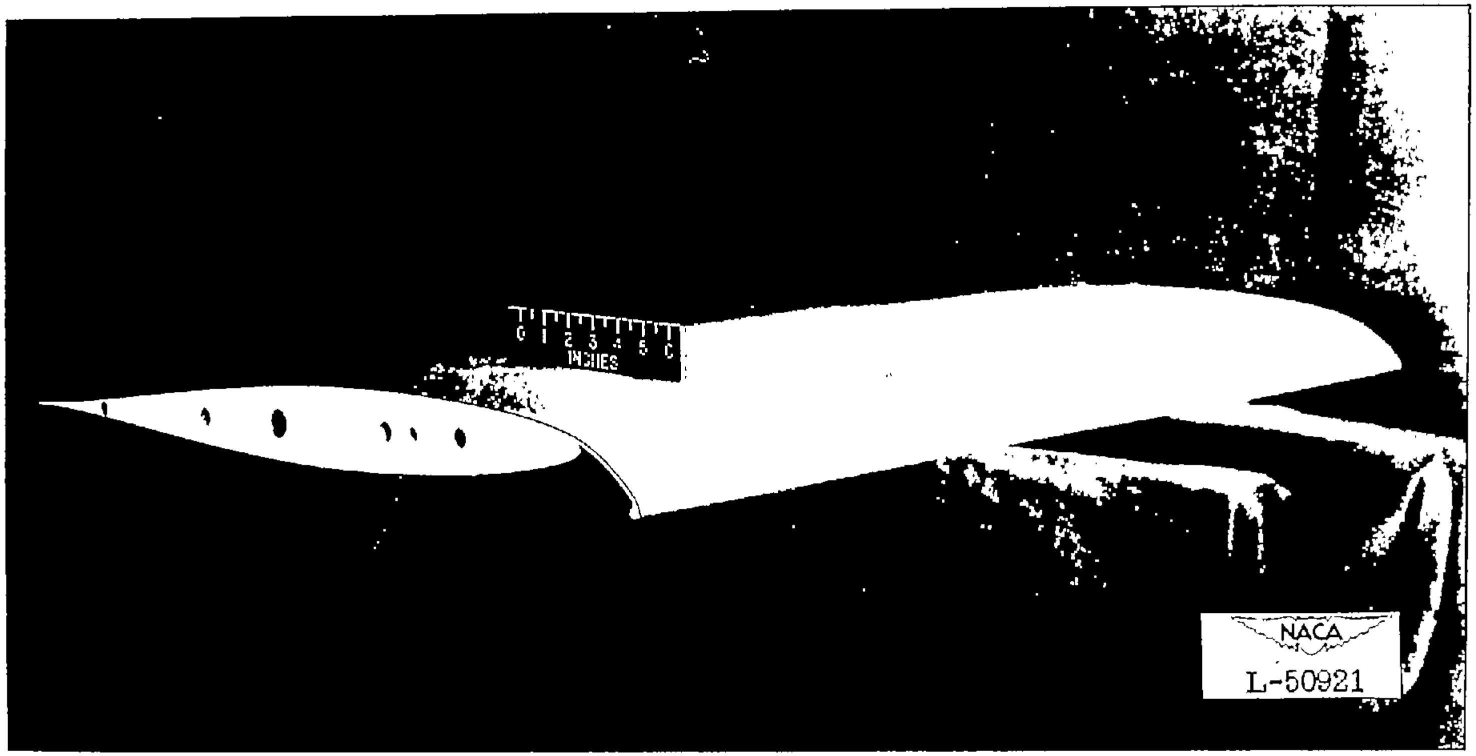

(b) Three-quarter front view of the model showing the contour of the upper-surface leading-edge flap.

Figure 1.- Concluded.

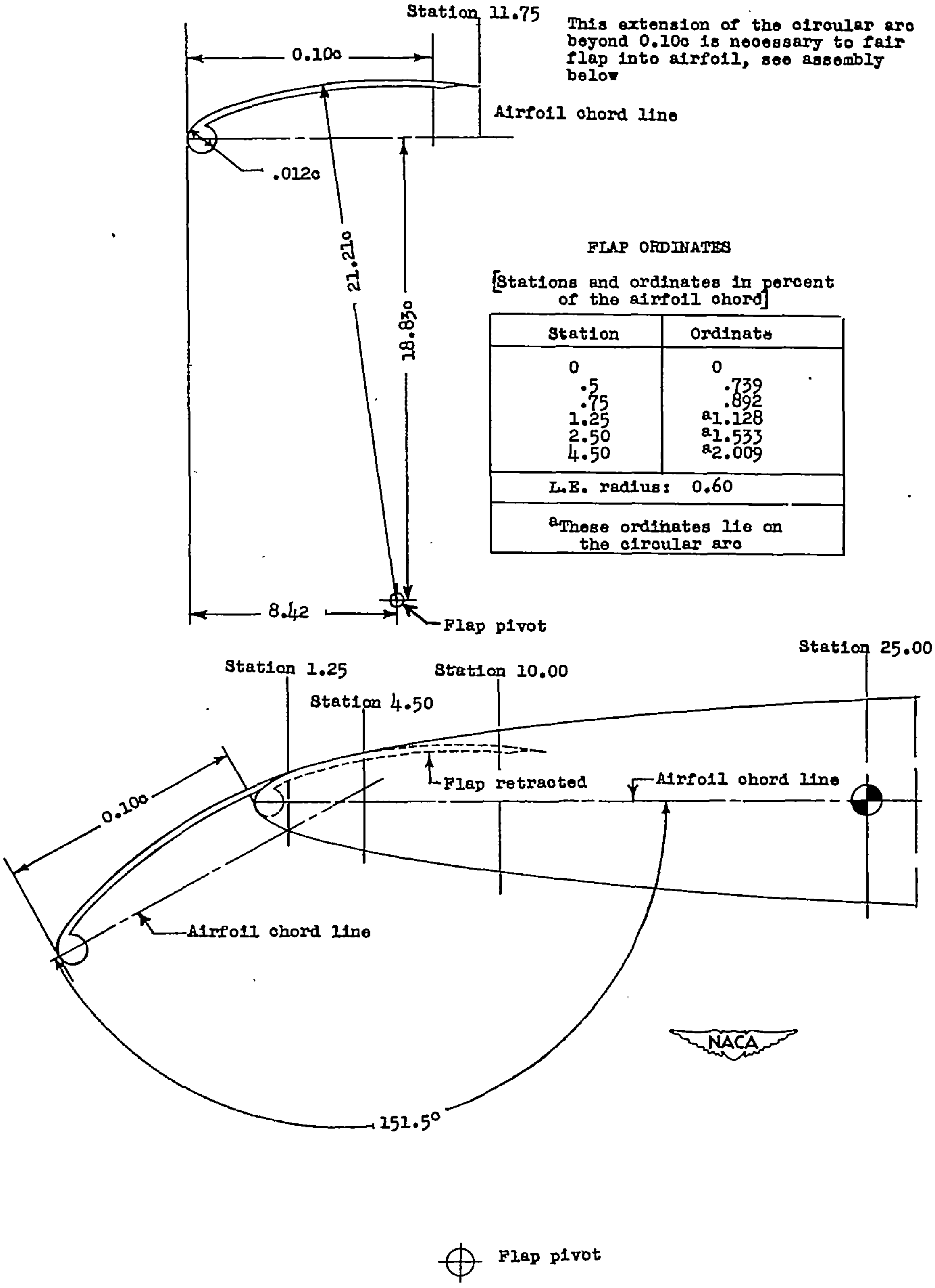

FLAP ORDINATES

[Stations and ordinates in percent of the airfoil chord]

Station	Ordinate
0	0
.5	.739
.75	.892
1.25	[a]1.128
2.50	[a]1.533
4.50	[a]2.009
L.E. radius: 0.60	

[a]These ordinates lie on the circular arc

Figure 2.- Sketch showing the upper-surface leading-edge flap, flap ordinates, and the arrangement of the flap on the NACA 64-009 airfoil section.

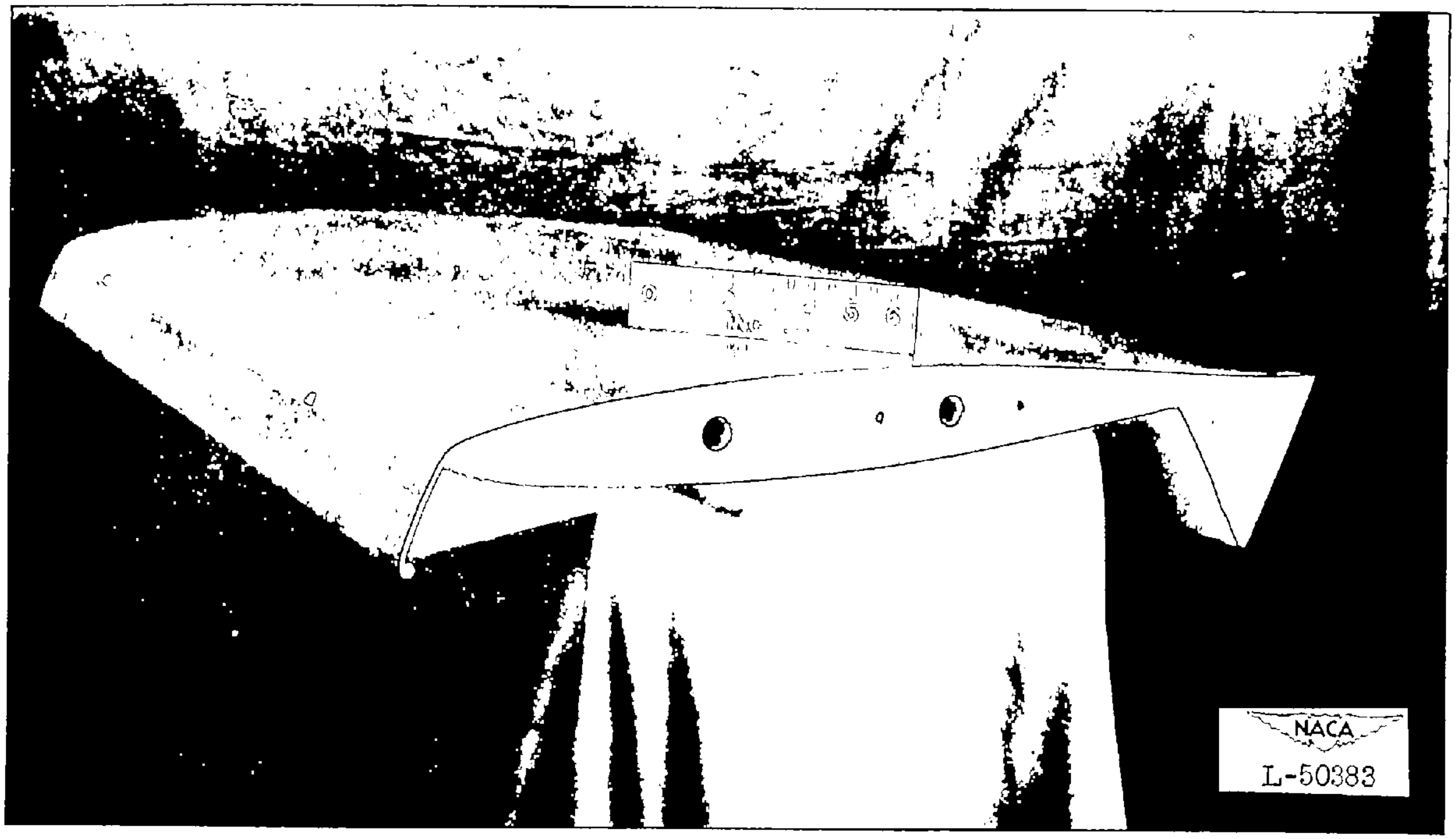

(a) Three-quarter front view of the model with leading-edge roughness showing the installation of the leading-edge and trailing-edge flaps.

Figure 3.- Photographs of the NACA 64-009 airfoil section with the 0.10c lower-surface leading-edge flap alone and in combination with the 0.20c trailing-edge split flap.

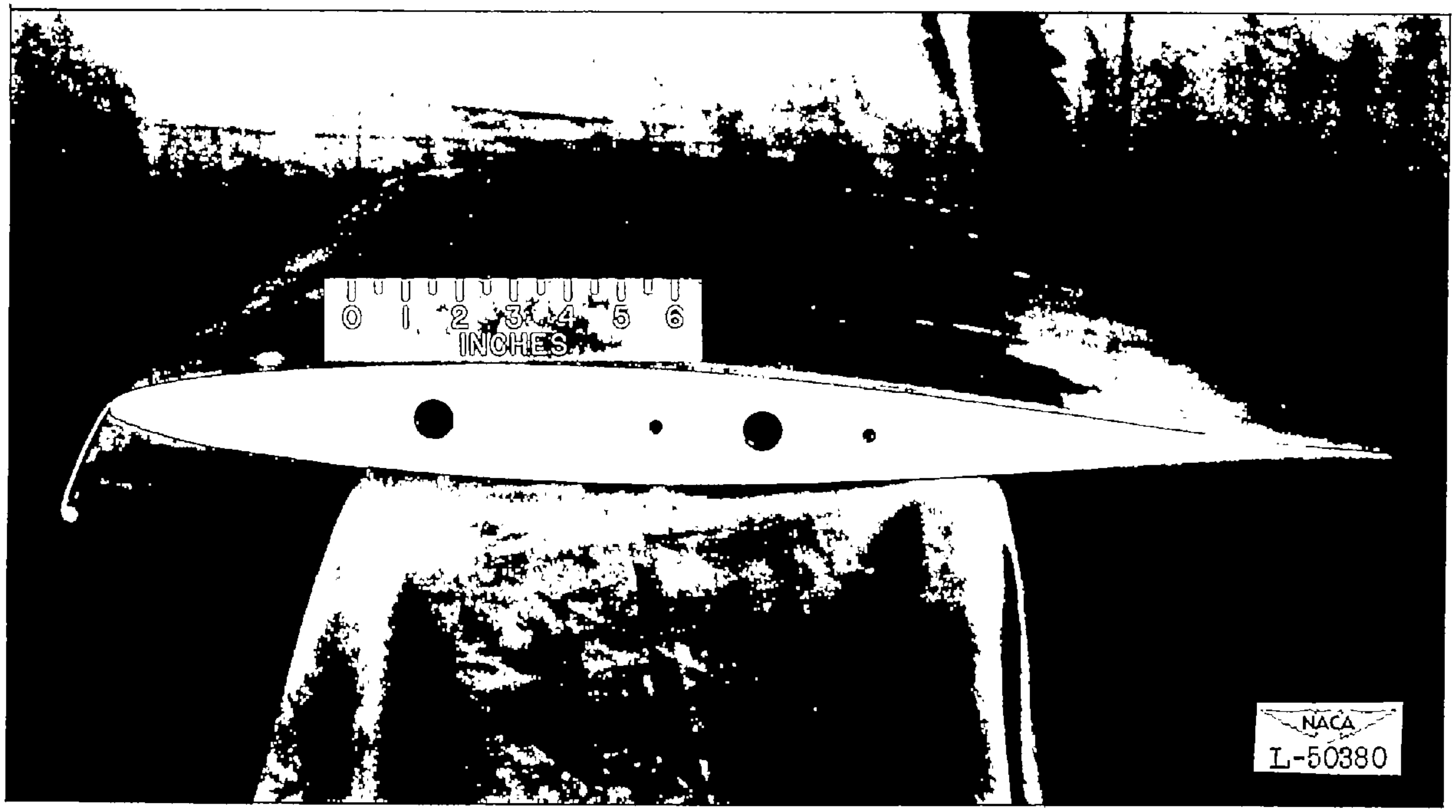

(b) Side view of the model showing the contour of the lower-surface leading-edge flap.

Figure 3.- Concluded.

Location of flap on airfoil

$\delta_{f_{L.E.}}$ (deg)	A (percent c)
0	0
100	.24
110	.26
120	.30
135	.34

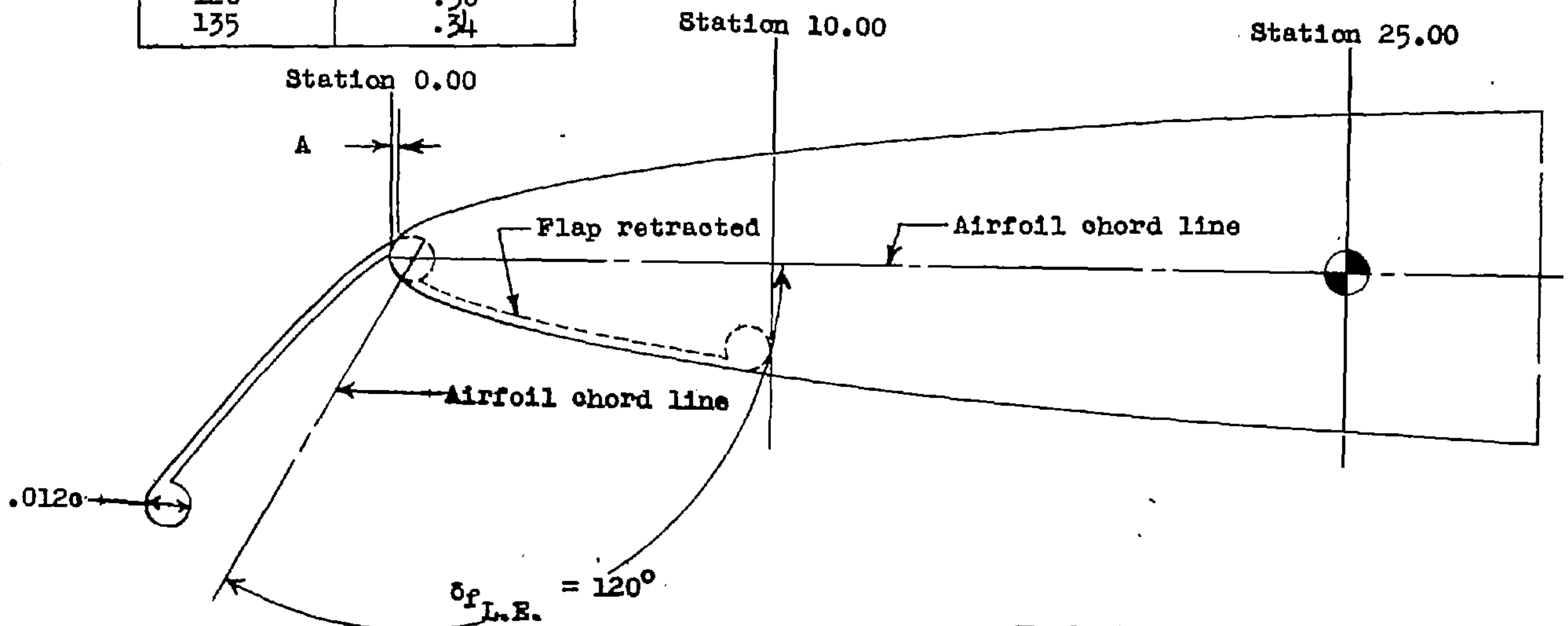

Figure 4.- Sketch showing the lower-surface leading-edge-flap arrangement on the NACA 64-009 airfoil section.

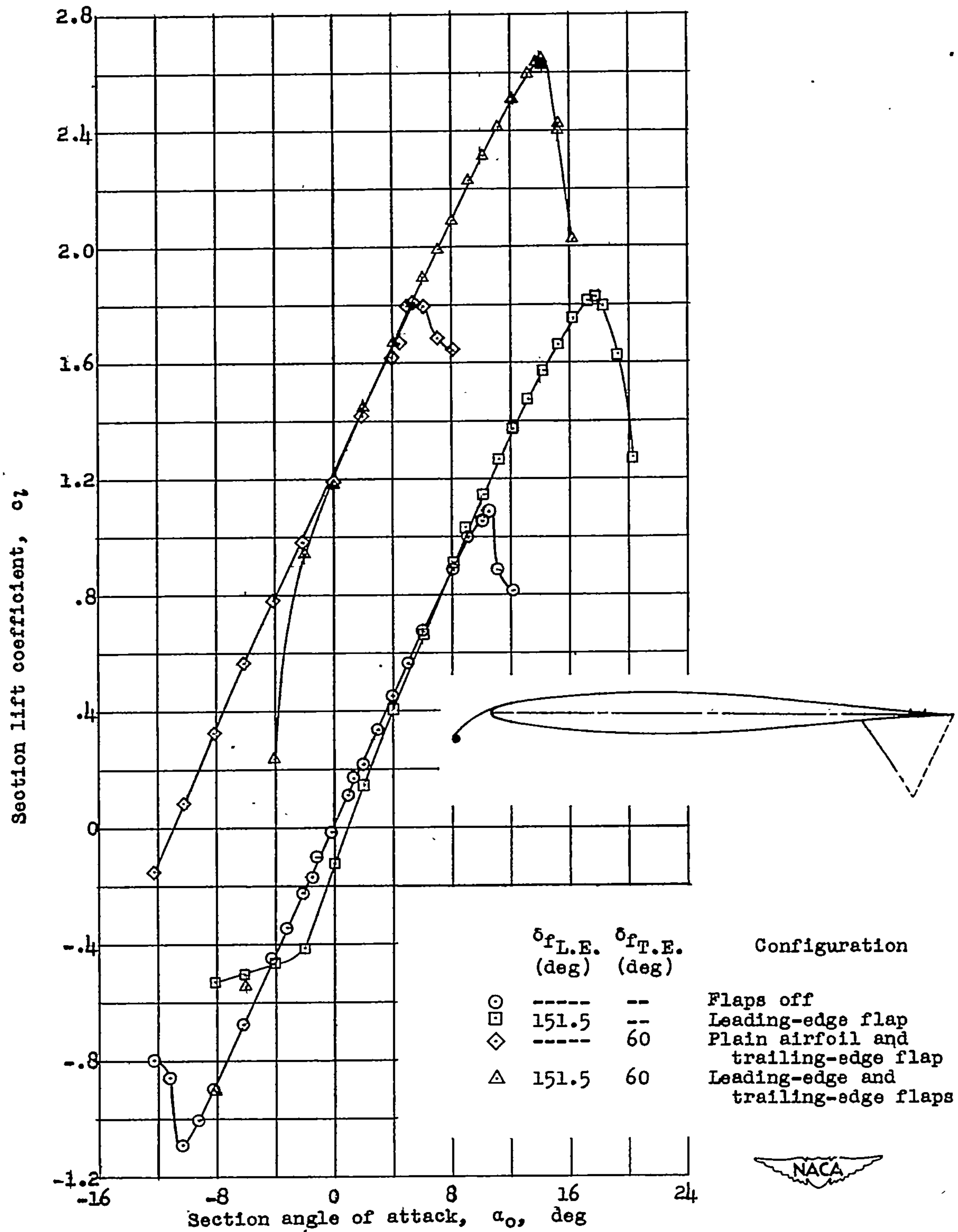

Figure 5.- Section lift characteristics for the NACA 64-009 airfoil section equipped with a 0.10c upper-surface leading-edge flap alone and in combination with a 0.20c trailing-edge flap. $R = 6.0 \times 10^6$.

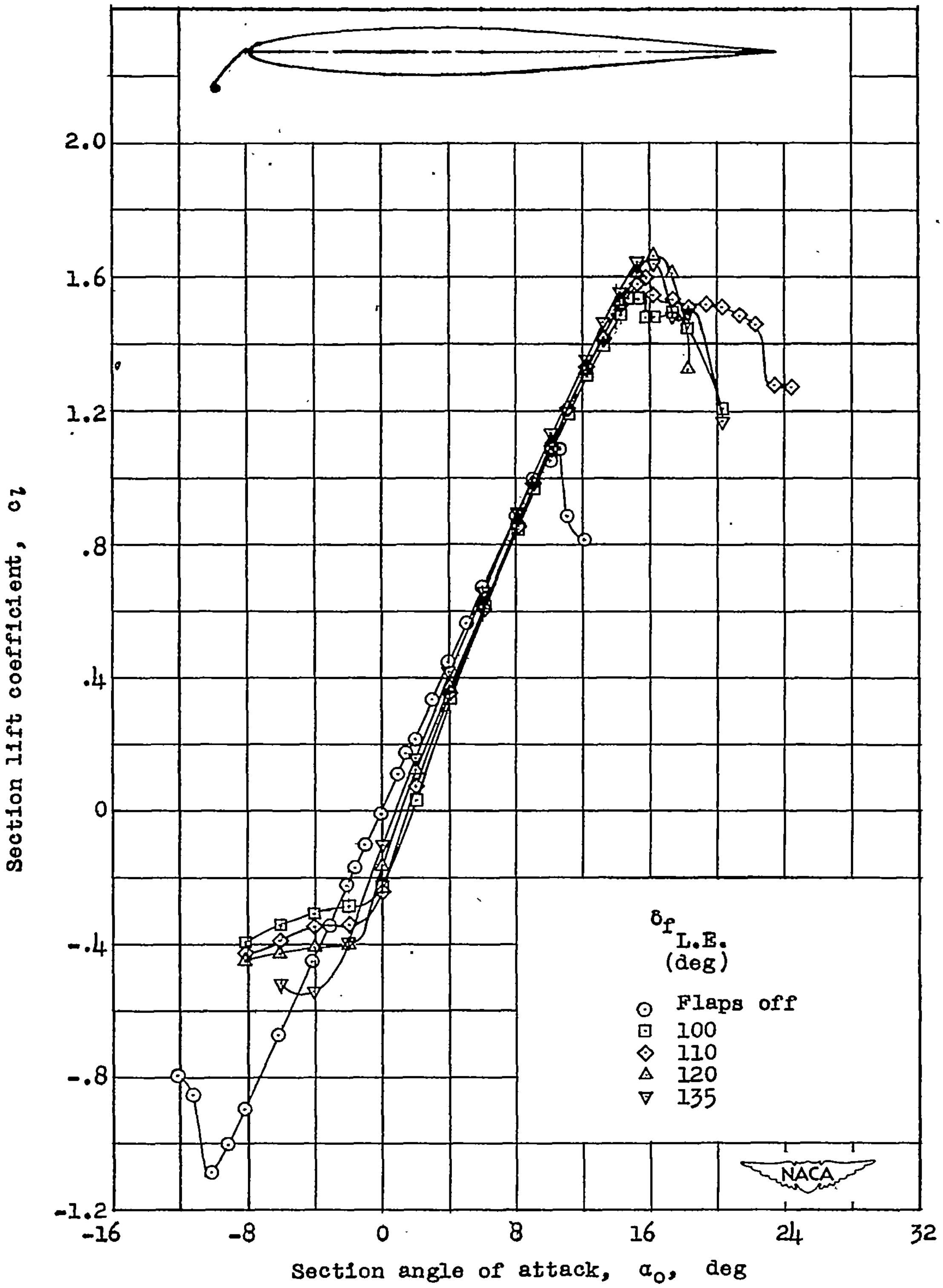

Figure 6.- Section lift characteristics for the NACA 64-009 airfoil section equipped with a 0.10c lower-surface leading-edge flap. $R = 6.0 \times 10^6$.

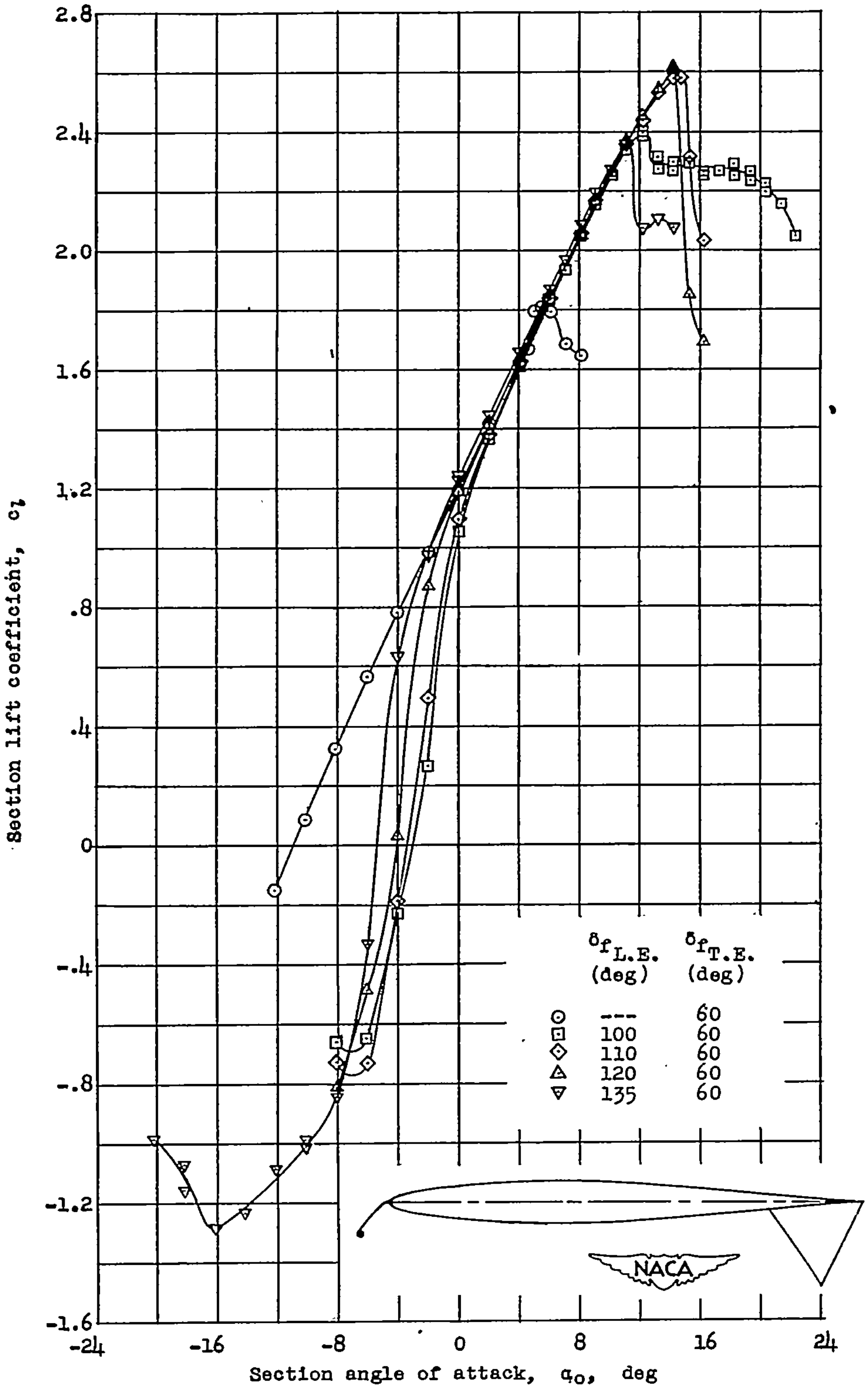

Figure 7.- Section lift characteristics for the NACA 64-009 airfoil section equipped with a 0.10c lower-surface leading-edge flap and a 0.20c trailing-edge flap. $R = 6.0 \times 10^6$.

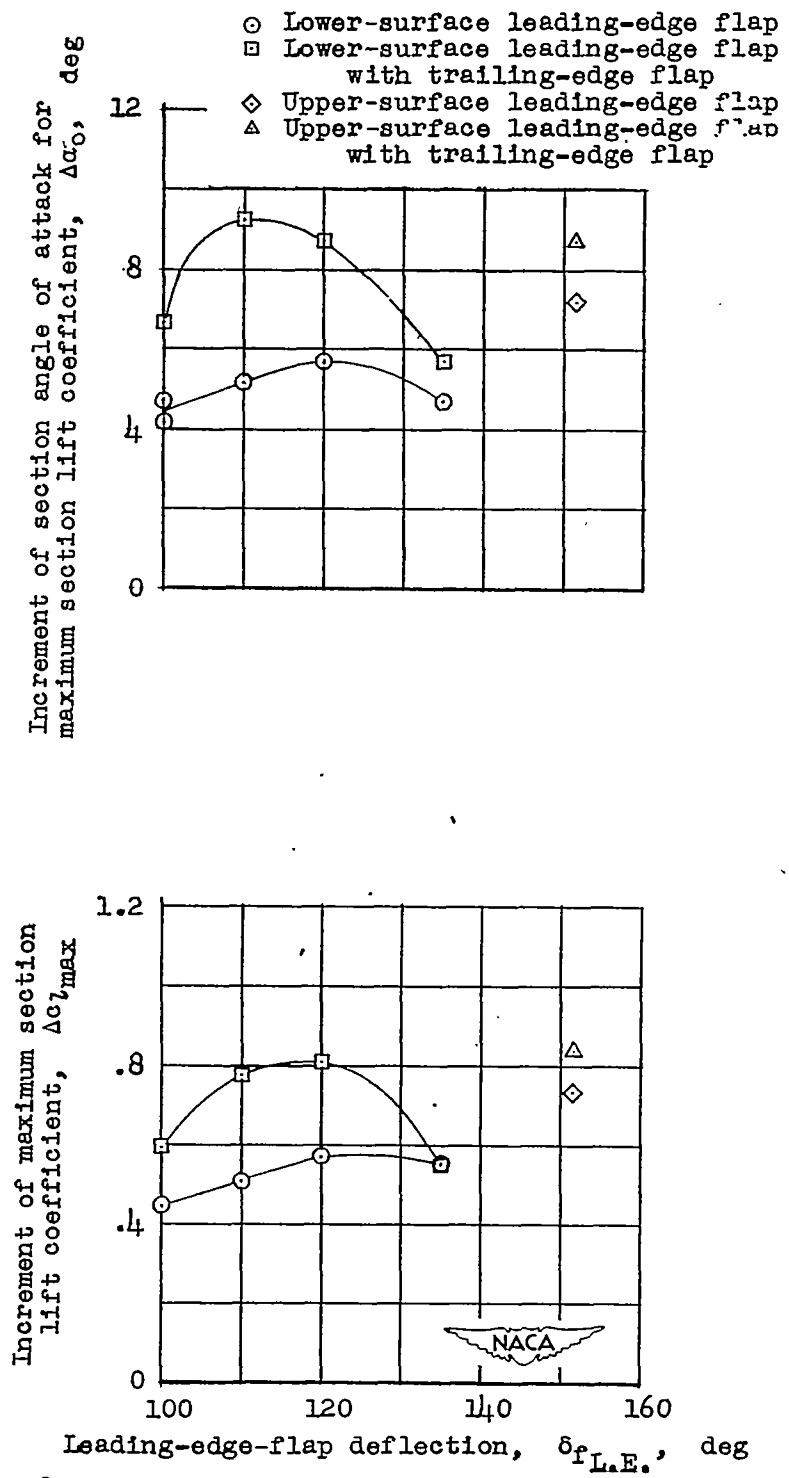

Figure 8.- Variation of the increment of maximum section lift coefficient and of the increment of section angle of attack for maximum section lift coefficient with leading-edge-flap deflection. NACA 64-009 airfoil section with various arrangements of leading-edge and trailing-edge flaps. $R = 6.0 \times 10^6$.

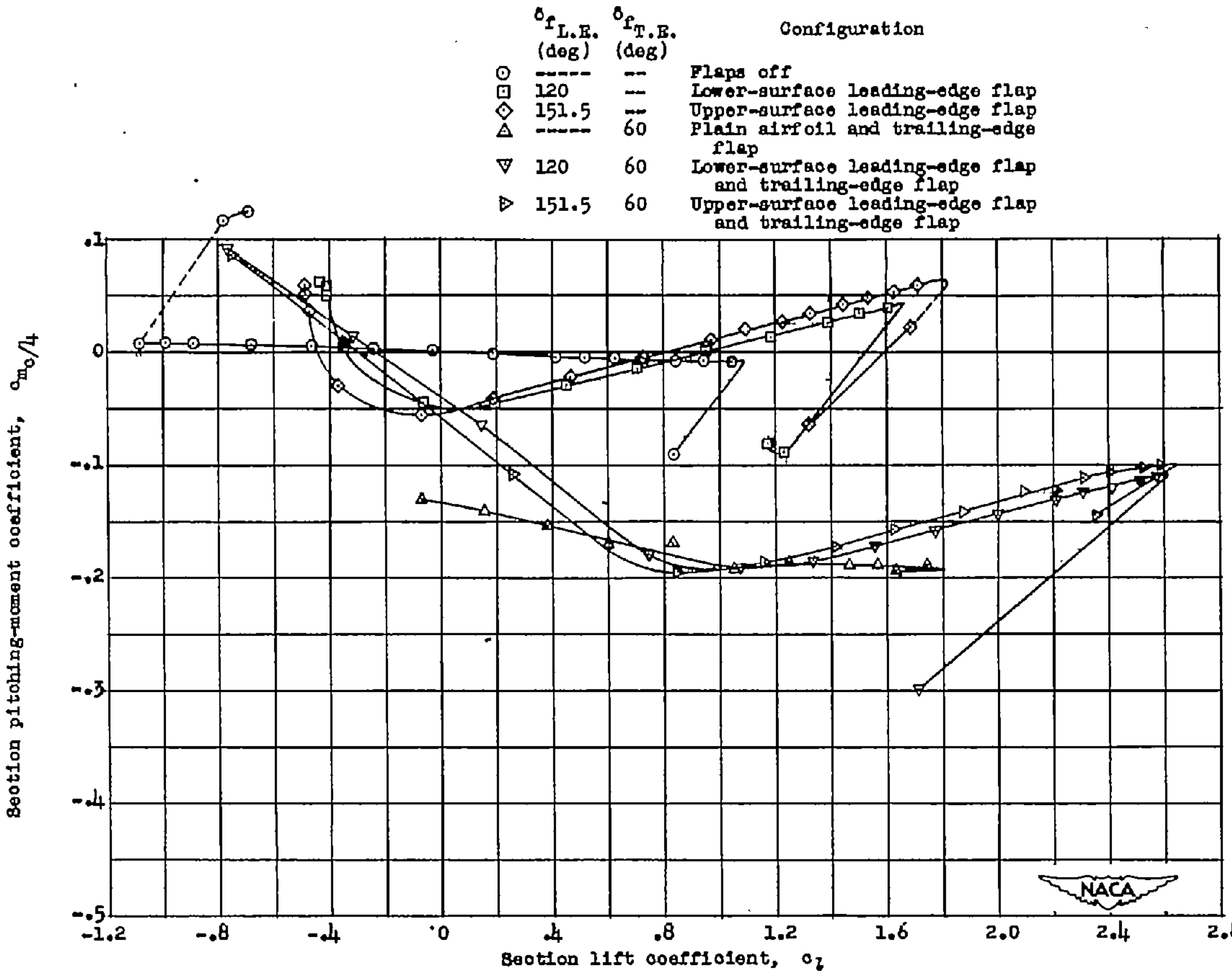

Figure 9.- Section pitching-moment characteristics for the NACA 64-009 airfoil section with various arrangements of leading-edge and trailing-edge flaps. $R = 6.0 \times 10^6$.

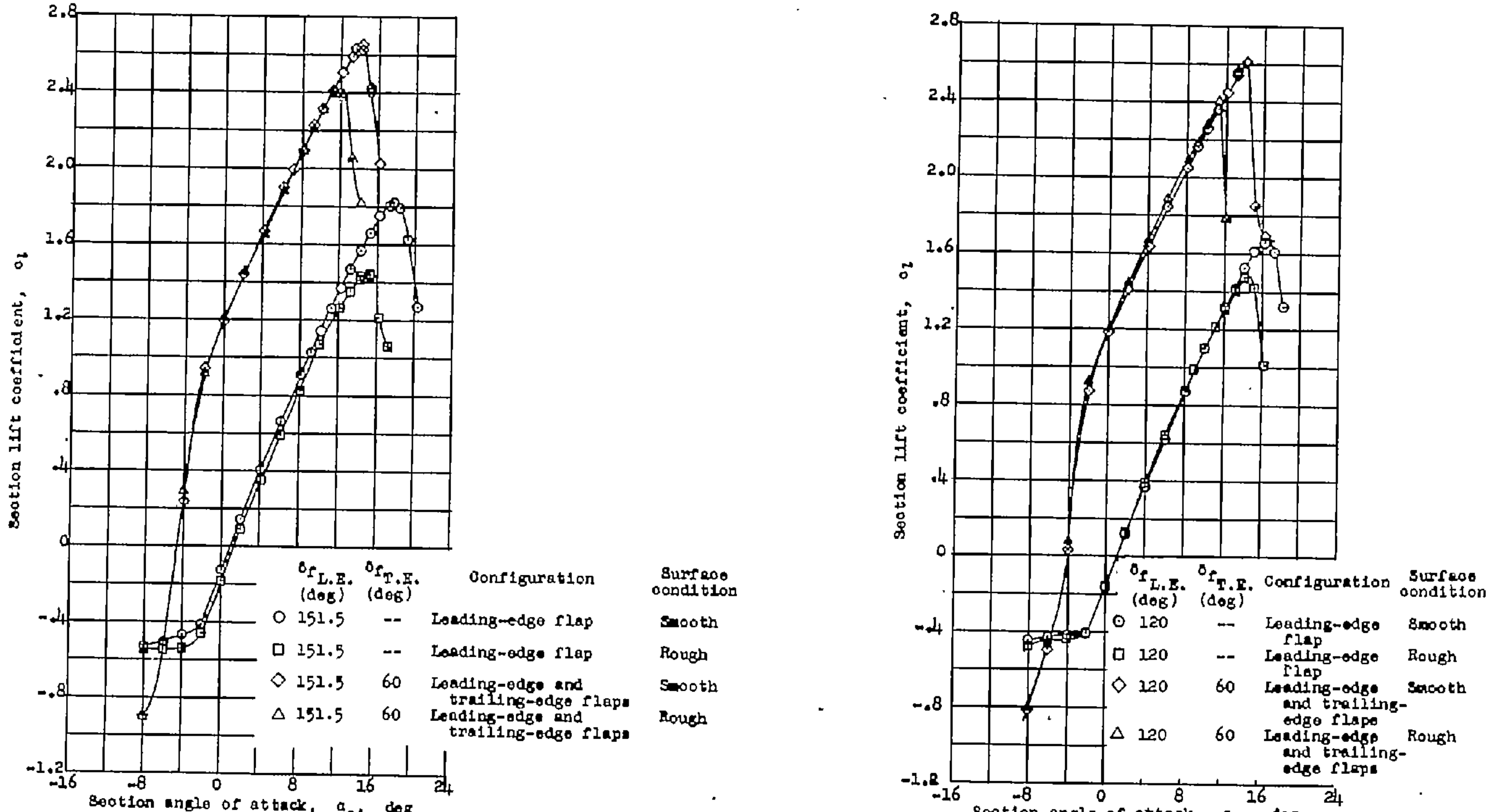

(a) Upper-surface leading-edge flap.

(b) Lower-surface leading-edge flap.

Figure 10.- The effect of leading-edge roughness on the section lift characteristics of the NACA 64-009 airfoil section with various arrangements of leading-edge and trailing-edge flaps. $R = 6.0 \times 10^6$.

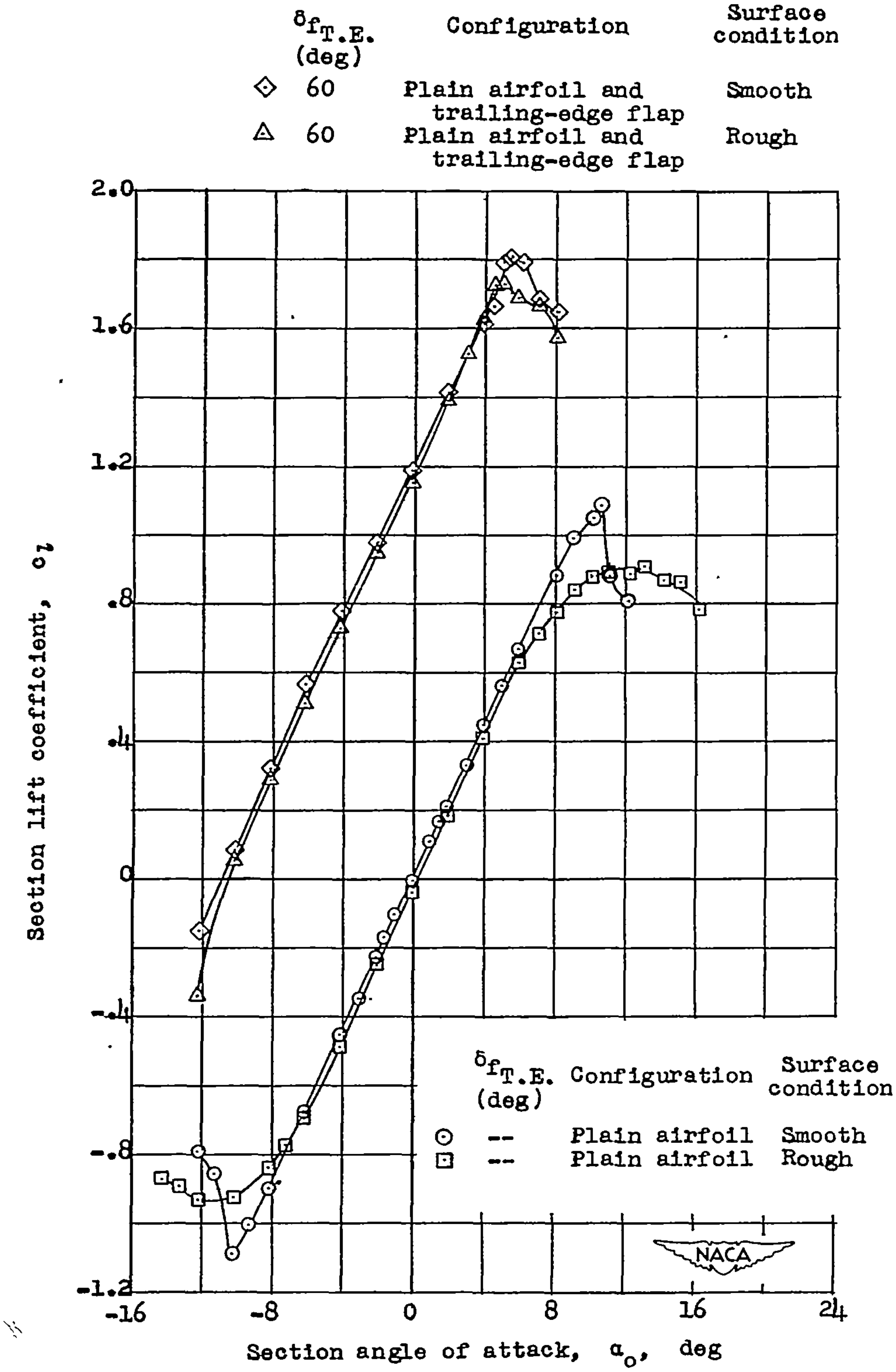

(c) Plain airfoil alone and with the trailing-edge flap.

Figure 10.- Concluded.